Computational and Theoretical Chemistry 963 (2011) 191–199

Contents lists available at ScienceDirect

Computational and Theoretical Chemistry

journal homepage: www.elsevier.com/locate/comptc

A B3LYP/6-31+G(d) study of the reaction pathways and conformational preference in a model Chichibabin reaction

Aleksandra Rudnitskaya, Béla Török, Timothy Dransfield *

Department of Chemistry, University of Massachusetts Boston, Boston, MA 02125, USA

ARTICLE INFO

Article history:
Received 12 July 2010
Received in revised form 13 October 2010
Accepted 13 October 2010
Available online 28 October 2010

Keywords:
Chichibabin reaction
DFT studies
Gaussian
Mechanism
Pyridines

ABSTRACT

The mechanism of the sodium amide initiated amination of pyridine, known as the Chichibabin reaction, was investigated at the B3LYP/6-31+G(d) level of theory. Although this reaction has been known for more than one hundred years, it remains a very useful and sometimes unique method for the synthesis of a variety of heterocyclic nitrogen-containing compounds. A total of six $S_N(A_E)$-based mechanistic pathways were proposed to explain the formation of the major product, α-aminopyridine, and the minor γ-byproduct. Our investigations showed that reaction pathways leading to both products proceed similarly. Our results showed that the most likely first step is the addition of sodium amide to either the alpha or the gamma position, then hydrogen gas elimination occurs, and finally the desired product forms in the work-up step. We found that the temperature and especially the nature of the solvent are critical factors in the reaction energy barriers and thus in obtaining reasonable yield for the preferred product. The alpha aminopyridine pathway is preferable to the gamma substitution when modeled regardless of temperature. The influence of the studied experimental conditions provides a reasonable explanation for the experimentally observed gamma byproduct. Based on the experimental evidence and our calculations, it is proposed that the mechanism proceeds through the loss of hydrogen gas rather than the formation of sodium hydride in the second step.

1. Introduction

The Chichibabin reaction was first reported in 1906 [1–10]. It may be described as the nucleophilic displacement of a hydride ion attached to a carbon atom of an aromatic nitrogen-containing heterocycle by an amino group. Originally, it was a method for preparation of α-aminopyridine by the reaction of pyridine with sodium amide [1–10]. The reaction was discovered unexpectedly by Chichibabin and Zeide and later was applied using many heterocycles such as pyridines, quinolines, isoquinolines, pyrazines, pyrimidines, pyridazines, naphthyridines, imidazoles, quinoxalines, quinazolines, triazines, purines, and many others [11–36]. The reaction has been influential in the development of heterocyclic chemistry and has become of great industrial importance as many aminopyridines are valuable intermediates, especially in the pharmaceutical industry [37–39]. Over the years a major focus of the research on the Chichibabin reaction was on how to improve the synthetic methods, rather than concentrating on mechanistic aspects. Thus the emphasis has shifted to achieving improved protocols that are inherently more environmentally friendly, resulting in the development of the so-called modified Chichibabin reaction [14–30]. This modified reaction is widely used as an intermediate step in many organic syntheses [31–39]. There has also been much interest of late in the modified Chichibabin reaction, due to the possible applications in area of chemosensors [41], and pyridine-containing polymers [40].

The Chichibabin reaction can be conducted under heterogeneous and homogeneous conditions in inert aprotic (e.g. toluene) and protic (NH_3) solvents at appropriate temperatures. Homogeneous conditions can be applied to the system when both reagents are completely dissolved in a solvent, while heterogeneous conditions are applicable when one of the reagents, usually sodium amide, does not dissolve in the solvent and the reaction occurs on the surface of the solid reagent. Gas production and the appearance of an intense red color are typical indications of the progress of the reaction. The mechanism is still not clearly understood, largely due to the difficulties involved with handling the highly reactive alkaline metal amides and with investigating reaction kinetics at higher temperatures. Therefore, computational methods are of high importance in the evaluation of the energetics of possible reaction pathways and kinetics to make important observations toward the better understanding of the reaction mechanism.

* Corresponding author.
E-mail address: Timothy.Dransfield@umb.edu (T. Dransfield).

2210-271X/$ - see front matter © 2010 Elsevier B.V. All rights reserved.
doi:10.1016/j.comptc.2010.10.023

There is a general agreement in the literature that the Chichibabin reaction proceeds through an addition-elimination mechanism, $S_N(AE)$ [42]. The hydrogen displacement in a heterocyclic compound by an amide ion is a special case of nucleophilic substitution of hydrogen specified by symbol SNH. An alternative mechanism SN(ANRORC) (Addition of the Nucleophile to the heterocycle, Ring Opening, and Ring Closure) was also described in the literature [42]. There is a general understanding that a multistep mechanism involving successive ring opening and ring closure is energetically significantly more demanding than the addition process, which was convincingly proven by direct experimental kinetic and gas evolution studies [43]. Another possible pathway, the so-called pyridine pathway that involved the proposed formation of a C–C triple bond, was ruled out by Abramovitch based on the lack of isotope effect in the reaction [44]. Therefore, we decided not to consider these alternative mechanisms in the present study. Later still an autocatalytic pathway was considered that was supported by experimental result [45]. However, while being important steps in determining a most probable mechanism, the experiments in these studies were carried out in the heterogeneous phase, and thus involve surface phenomena and are not directly transferable to the present study. In our search for the most probable mechanistic pathway we concentrate on the investigation of the homogeneous mechanism due to several reasons. The reaction occurs with much higher yield in liquid ammonia, and thus it was determined that the system could best be treated without incurring the computational difficulties that arise during the handling of a heterogeneous reagent and surface-driven reaction.

Herein, we describe a DFT study of the most likely mechanisms of the S_NH pathway with the major goal of describing the elementary steps of the reaction. One ultimate goal is to identify if hydrogen gas formation is an important step, or if the reaction proceeds through sodium hydride formation and hydrogen gas is produced later as a result of the interaction of aminopyridine with sodium amide. Similar reactions may also prove to be of importance in the amination of nitrogen-containing heterocycles under milder conditions. Based on literature evidence and earlier experimental data, we have proposed, computed, and analyzed four detailed mechanistic descriptions for the reaction. During the calculations

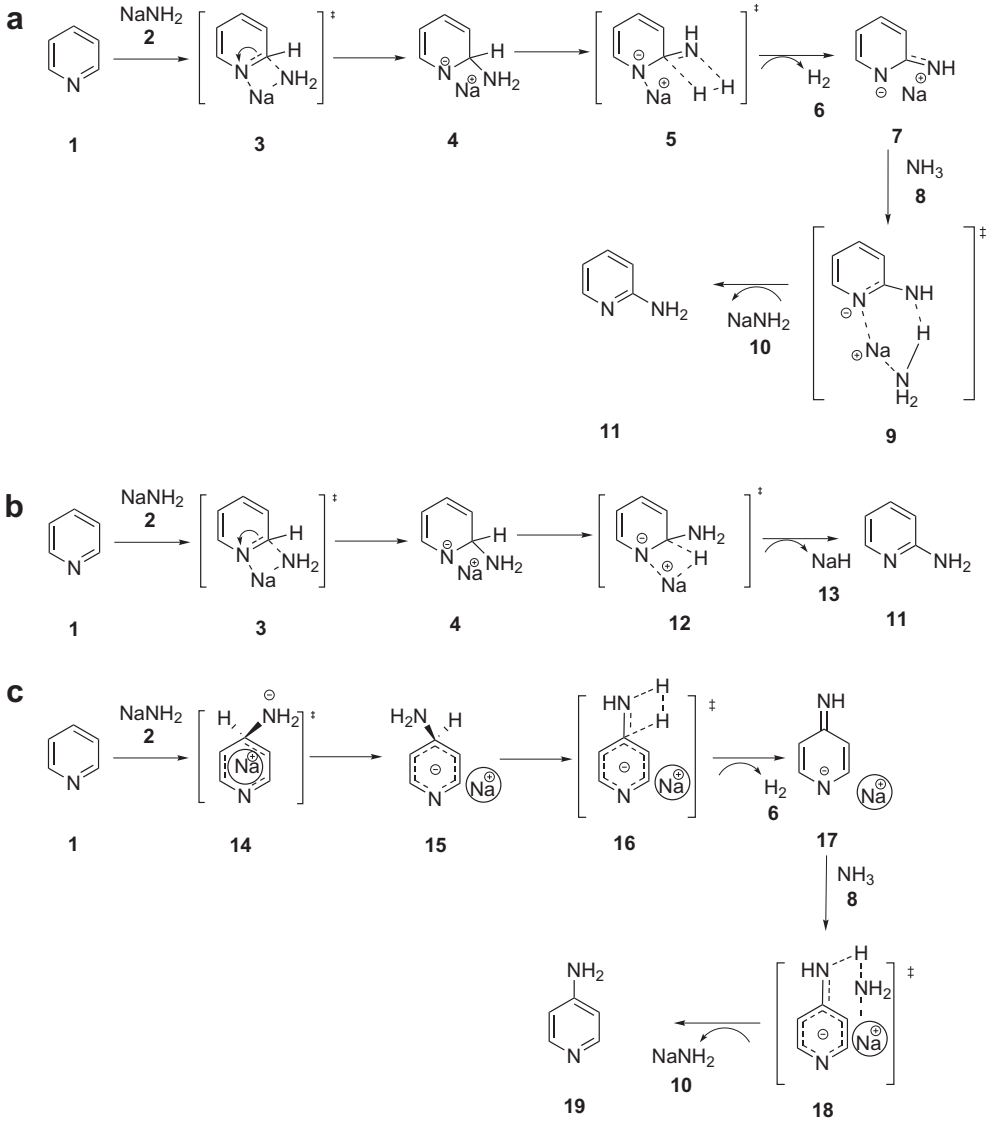

Scheme 1. Proposed mechanistic pathways for the Chichibabin reaction. The geometries and energies of all of the relevant species can be found in the Supplemental information. (a) Mechanism 1α; (b) mechanism 2α; (c) mechanism 1γ-*cis*; (d) mechanism 1γ-*trans*; (e) mechanism 2γ-*cis*; (f) mechanism 2γ-*trans*.

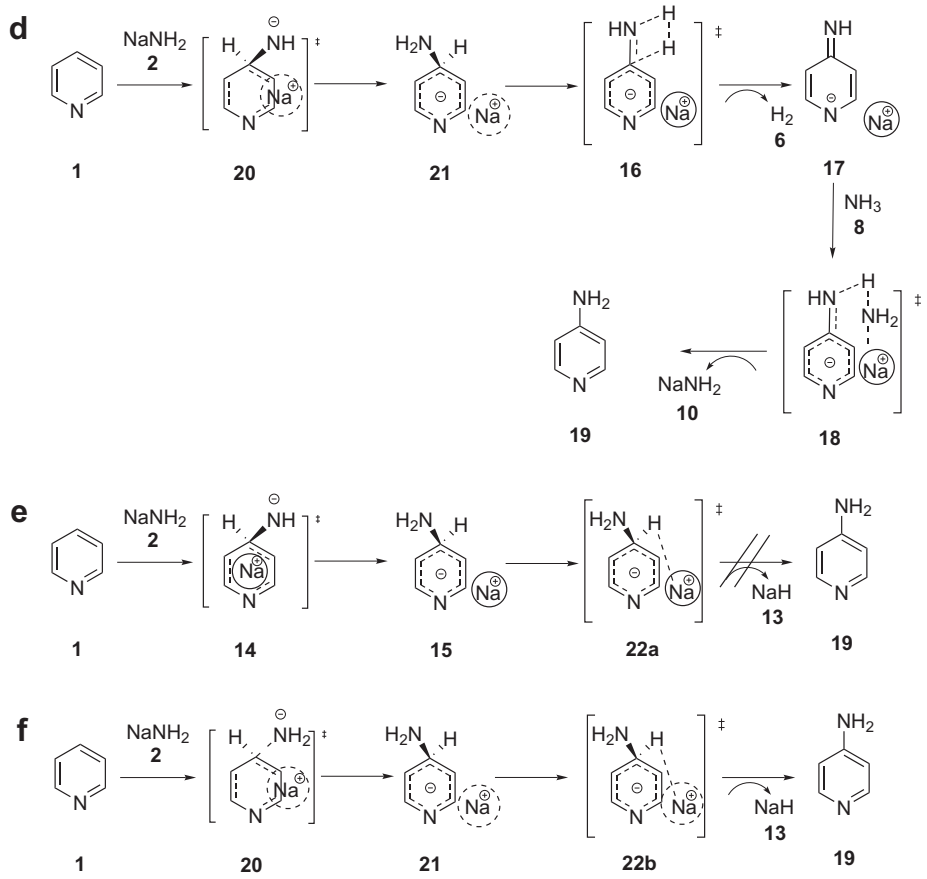

Scheme 1 (*continued*)

a broad temperature range was considered and applied in the computational studies.

2. Computational procedure

All calculations reported here were performed with the Gaussian03 computer software package [46]. Computations were run on the TeraGrid network at the National Center for Supercomputing Applications, on either an Silicon Graphics Instruments Altix (Cobalt) or an Intel 64 node cluster (Abe) [47]. After all geometry optimizations were performed, analytical vibration frequencies were calculated at the same level to determine the nature of the located stationary points. Thus all stationary points found were characterized by evaluation of the harmonic frequencies. Due to the nature of interacting species in the system and the absence of weak interactions, all calculations were performed on all reactants, products, and transition states using Becke's three-parameter hybrid method employing the LYP correction functions (B3LYP), in conjunction with the split valence polarized basis set, 6-31+G(d). The single-point energies of all the stationary points and the energy barriers of the sum of the electronic and thermal enthalpies were calculated at this same level, with scaled zero-point vibration energies included. A scaling factor of 0.9611 for zero-point vibrational energies was used [48].

A series of DFT calculations using the same B3LYP/6-31+G(d) method was performed to identify the equilibrium structures (ES) and transition states (TS) during the synthesis of pyridine derivatives. Harmonic vibrational frequency calculations of the stationary points were performed at the same level of theory. The energies and geometries of pyridine, α- and γ-aminopyridine, and all other stable species were obtained by an energy minimization and were characterized by a local energy minimum on the energy surface and by the absence of imaginary frequencies in the predicted vibrational spectra. Characteristics and geometries of transition states (TS) were confirmed by the existence of only one imaginary frequency corresponding to the expected transition vector.

Calculations involving an ammonia solvent were conducted using the Self-Consistent Reaction Field (SCRF) method with the Isodensity Polarized Continuum Model (IPCM) at the same level of theory. This method calculates the electric field analytically and defines a cavity in the solvent based on an isosurface of the total electron density of the solute, calculated at the level of theory being applied [48]. The solvent effects are thus derived from the interaction of the potential isosurface with the dielectric continuum. For our system we introduced protic polar solvent liquid ammonia with dielectric constant $\varepsilon = 16.030$. All stationary points obtained in the gas-phase calculations were re-optimized using the SCRF method. The effect of temperature was studied in the gas phase over the range 293.15–473.15 K with gradual increase in 20 K increments, which is a typical interval for experimental procedures [42].

3. Results and discussion

As described above, all studied pathways are considered to be of the S_NH type. There are two major steps; the formation of σ-adducts, and the elimination process. An ionic σ-adduct, or Meisen-

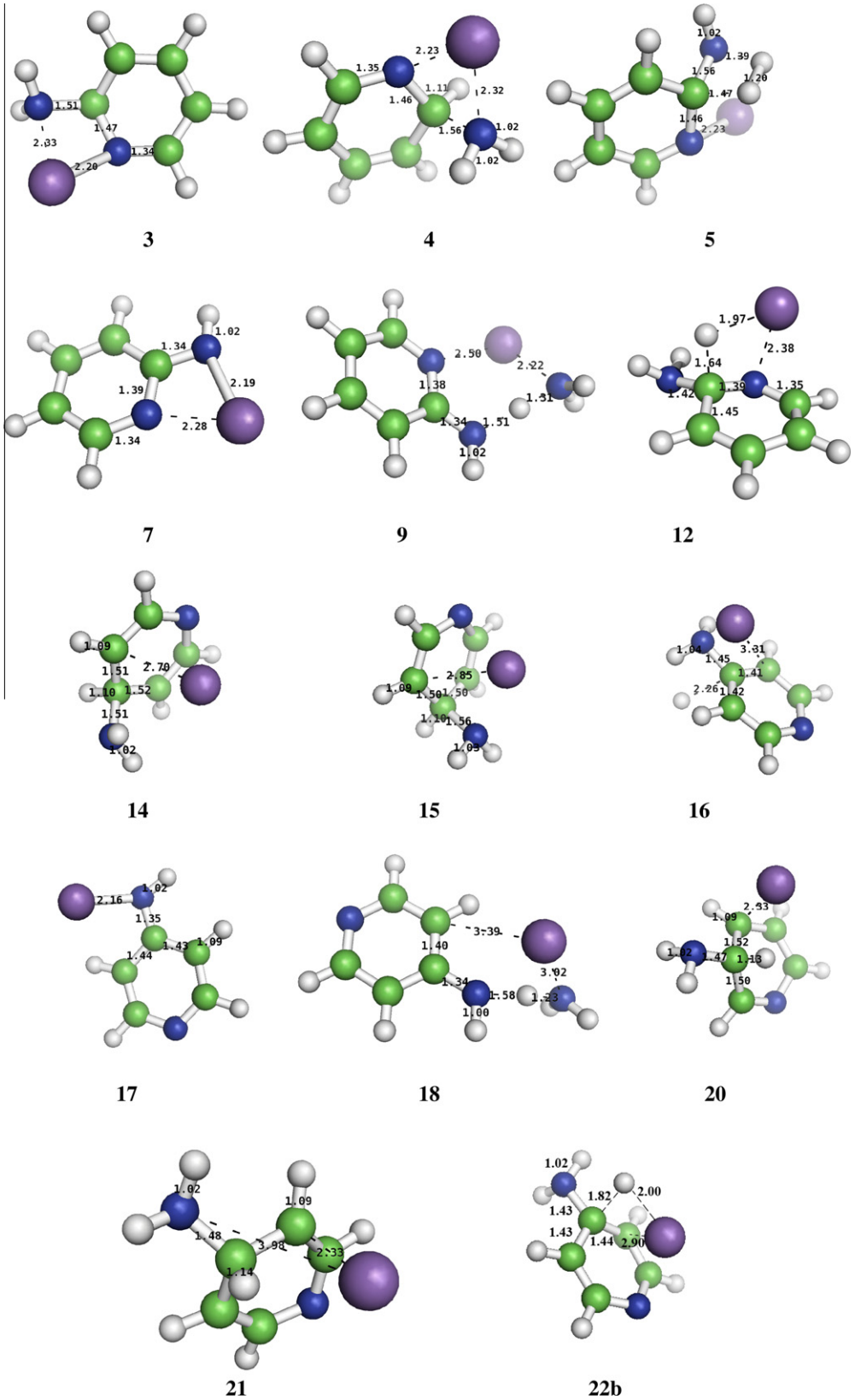

Fig. 1. Graphical representation of optimized intermediate and transition state structures proposed during the formation of the α-product: **3**; **4**; **7**; **5**; **9**; **12**; and for the formation of γ-product: **14**; **15**; **16**; **17**; **18**; **19**; **20**; **21**; **22** (*color code:* H – white; N – blue; C – green; Na – purple). (For interpretation of the references to color in this figure legend, the reader is referred to the web version of this article.)

heimer-complex, was characterized by the formation of a new σ-bond between the nucleophile and a ring carbon atom of pyridine. The aromaticity of the ring is disrupted in this process. The existence of σ-adduct intermediates (**4**), (**15**), and (**21**) (Scheme 1)

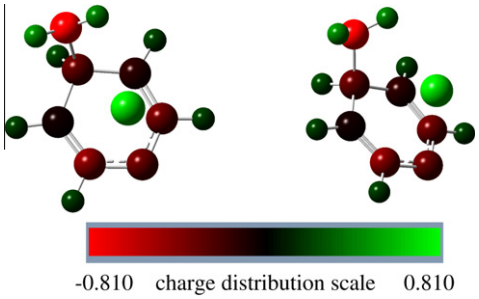

Fig. 2. Electron density of **14**.

have been proven experimentally via their isolation and characterization by ^{1}H- and ^{13}C-NMR spectroscopy [49], and IR, ESR spectroscopy [48] in the reaction of pyridine and similar nitrogen-containing heterocycles. Under homogeneous conditions, the σ-adducts of electron-deficient heterocycles form very easily and rapidly, even at low temperatures. The elimination step and its products are different and depend on the proposed mechanism. In this work we propose two major mechanistic pathways that are fundamentally different in the elimination steps, which proceed via either hydrogen gas (mechanism 1) or sodium hydride production (mechanism 2). The detailed proposed pathways (Scheme 1) take into account the regioselectivity of the reaction, namely the formation of α- and γ-substituted products.

We observe that, while there are quantitative differences between our computed gas-phase results and those of the implicit solvent calculations, there are no substantial qualitative differences. The barrier heights calculated in the gas phase are generally 2.0–6.0 kCal/mol higher than those obtained from calculations with the solvent. Energies of stable species vary less significantly, by 1.0–1.5 kCal/mol.

Mechanisms 1α and 2α were designed to explain the formation of α-aminopyridine while mechanisms 1γ-*cis*, 1γ-*trans* and 2γ-*cis*, 2γ-*trans* attempted to rationalize γ-aminopyridine formation. Pathways 1α, 1γ-*cis*, 1γ-*trans* and 2α, 2γ-*cis*, 2γ-*trans* have similar approaches. As shown in Scheme 1, there is only one possibility for an attack in the α position: the Na^{+}-ion is located near the N atom of the ring that would bear the negative charge. In contrast, there are two steric alternatives for the γ-substitution. Upon attacking the ring, the NH_2-ion will take a position on one side of the aromatic ring, on the newly formed sp^3 type carbon. The sodium cation can be located either on the same side (*cis* pathway) or the opposite side of the ring (*trans* pathways). We have conducted an extensive analysis of several of the proposed transition states and intermediates. In addition, we have considered alternatives as well. While in most cases the proposed processes in Scheme 1 allow no alternative structures, mechanisms 1γ-*cis*, 1γ-*trans*, 2γ-*cis* and 2γ-*trans* include species where the question arises as to whether the sodium ion is quasi-covalently bound to any particular carbon of the ring, or whether a more homogeneous electron distribution should be taken into account for the pyridine ring, which would dislocate the Na^{+} from a well-defined carbon and suggest a non-covalent interaction between the negative charge delocalized on the ring and the cation. The structures of several such species are summarized in Fig. 1.

The optimized geometries for transition states involved in mechanisms 1γ-*cis*, 1γ-*trans*, 2γ-*cis* and 2γ-*trans* indicate that

Table 1
The activation energy barriers (E_a) and enthalpies (ΔH) of the steps of the reaction calculated at different temperatures, in kCal/mol. In bold given energies under experimental temperature.

T (K)		Mech 1α	Mech 2α	Mech 1γ-*cis*	Mech 1γ-*trans*	Mech 2γ-*trans*		Mech 1α	Mech 2α	Mech 1γ-*cis*	Mech 1γ-*trans*	Mech 2γ-*trans*
293.15	E_{a1}	0.9	0.9	4.0	58.6	58.6	ΔH_1	−0.2	−0.2	−2.2	−5.7	−5.7
	E_{a2}	12.3	24.1	18.2	18.2	2.8	ΔH_2	−12.9	−0.7	−2.8	−2.8	−4.6
	E_{a3}	16.0		11.7	11.7		ΔH_3	−5.5		−3.7	−3.7	
313.15	E_{a1}	0.9	0.9	3.9	58.6	58.6	ΔH_1	−0.2	−0.2	−2.2	−5.7	−5.7
	E_{a2}	12.3	24.1	18.1	18.1	2.8	ΔH_2	−12.7	−0.5	−2.8	−2.8	−4.6
	E_{a3}	16.0		11.7	11.7		ΔH_3	−5.4		−3.6	−3.6	
333.15	E_{a1}	0.8	0.8	3.9	58.5	58.5	ΔH_1	−0.2	−0.2	−2.2	−5.7	−5.7
	E_{a2}	12.3	24.1	18.0	18.0	2.8	ΔH_2	−12.7	−0.4	−2.9	−2.9	−4.5
	E_{a3}	16.0		11.7	11.7		ΔH_3	−5.4		−3.6	−3.6	
353.15	E_{a1}	0.8	0.8	3.9	58.5	58.5	ΔH_1	−0.3	−0.3	−2.2	−5.7	−5.7
	E_{a2}	12.3	24.1	17.8	17.8	2.8	ΔH_2	−12.6	−0.3	−3.0	−3.0	−4.5
	E_{a3}	16.0		11.7	11.7		ΔH_3	−5.4		−3.6	−3.6	
373.15	E_{a1}	0.8	0.8	3.9	58.5	58.5	ΔH_1	−0.3	−0.3	−2.2	−5.7	−5.7
	E_{a2}	12.3	24.1	17.7	17.7	2.8	ΔH_2	−12.5	−0.3	−3.0	−3.0	−4.5
	E_{a3}	16.0		11.7	11.7		ΔH_3	−5.4		−3.6	−3.6	
393.15	E_{a1}	0.8	0.8	3.9	58.5	58.5	ΔH_1	−0.3	−0.3	−2.2	−5.8	−5.8
	E_{a2}	12.3	24.1	17.6	17.6	2.8	ΔH_2	−12.5	−0.3	−3.1	−3.1	−4.5
	E_{a3}	16.0		11.7	11.7		ΔH_3	−5.3		−3.6	−3.6	
413.15	E_{a1}	**0.8**	**0.8**	**3.9**	**58.5**	**58.5**	ΔH_1	**−0.3**	**−0.3**	**−2.2**	**−5.8**	**−5.8**
	E_{a2}	**12.3**	**24.1**	**17.5**	**17.5**	**2.8**	ΔH_2	**−12.4**	**−0.3**	**−3.2**	**−3.2**	**−4.5**
	E_{a3}	**16.0**		**11.7**	**11.7**		ΔH_3	**−5.3**		**−3.6**	**−3.6**	
433.15	E_{a1}	0.7	0.7	3.9	58.5	58.5	ΔH_1	−0.3	−0.3	−2.3	−5.8	−5.8
	E_{a2}	12.3	24.1	17.4	17.4	2.8	ΔH_2	−12.4	−0.3	−3.3	−3.3	−4.5
	E_{a3}	15.9	0.0	11.7	11.7		ΔH_3	−5.3		−3.5	−3.5	
453.15	E_{a1}	0.7	0.7	3.9	58.5	58.5	ΔH_1	−0.4	−0.4	−2.3	−5.8	−5.8
	E_{a2}	12.3	24.1	17.3	17.3	2.8	ΔH_2	−12.3	−0.3	−3.3	−3.3	−4.5
	E_{a3}	15.9		11.7	11.7		ΔH_3	−5.3		−3.5	−3.5	
473.15	E_{a1}	0.7	0.7	3.9	56.9	56.9	ΔH_1	−0.4	−0.4	−2.3	−5.9	−5.9
	E_{a2}	12.3	24.1	17.0	17.0	2.8	ΔH_2	−12.3	−0.4	−3.4	−3.4	−4.5
	E_{a3}	15.9		11.7	11.7		ΔH_3	−5.3		−3.5	−3.5	

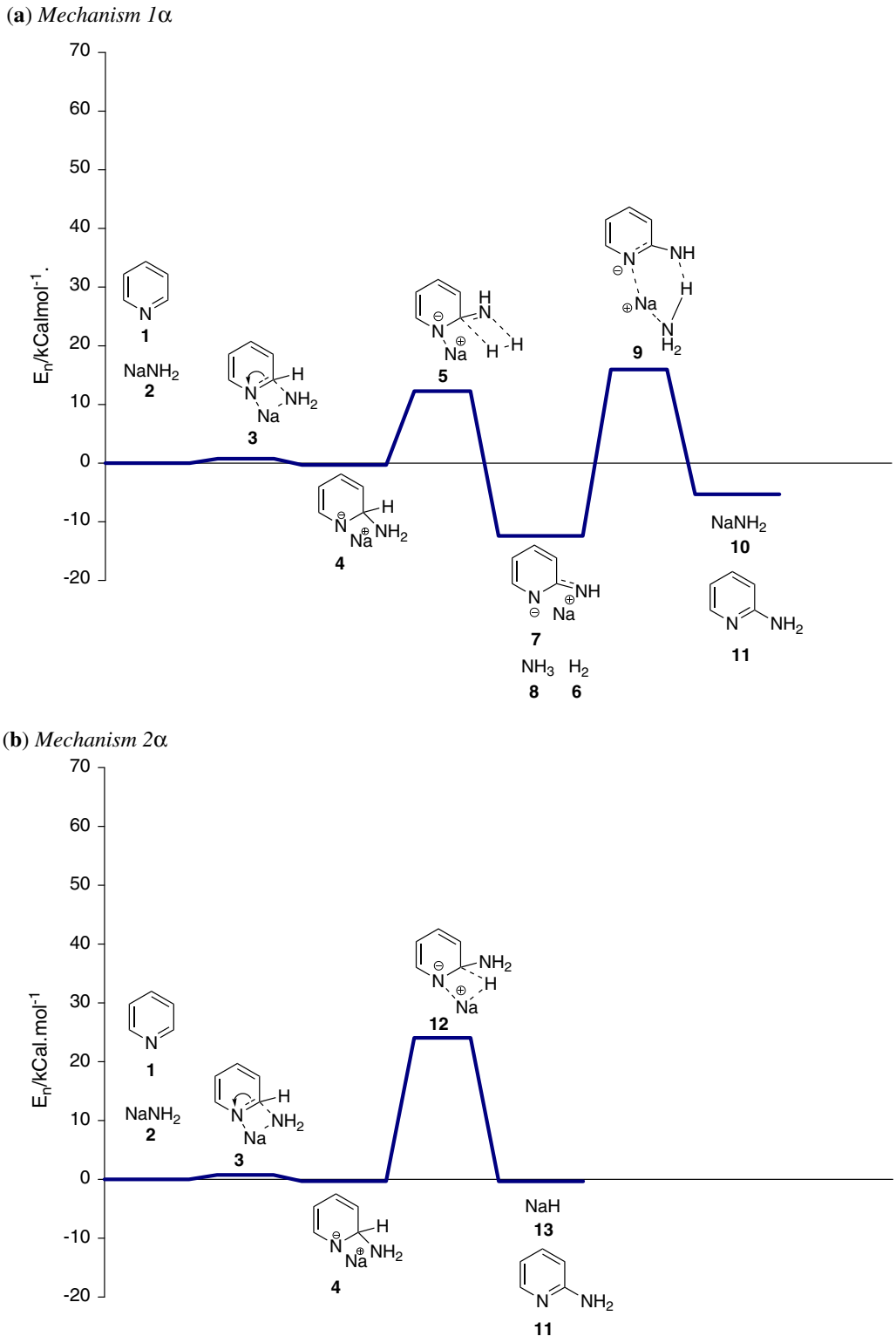

Fig. 3. Potential energy surface (PES) diagrams for the stepwise production of α-aminopyridine and byproducts (a), (b) and γ-aminopyridine and byproducts (c–e) (temperature 413.15 K).

the conventional covalent interaction between the sodium cation and the ring carbon atoms is highly unlikely, and that the delocalized species are energetically favored. These observations have been confirmed by the electrostatic potential representation of these species. The electron distribution in **14** is shown in Fig. 2.

Fig. 2 clearly shows that the ring atoms bear almost identical electron density, and negative charge indicating the delocalized nature of the aromatic electrons in this transition state species. Thus, we conclude that it is not reasonable to suggest covalently bound Na^+ cations and propose non-covalently bound sodium

(**c**) *Mechanism 1γ cis*

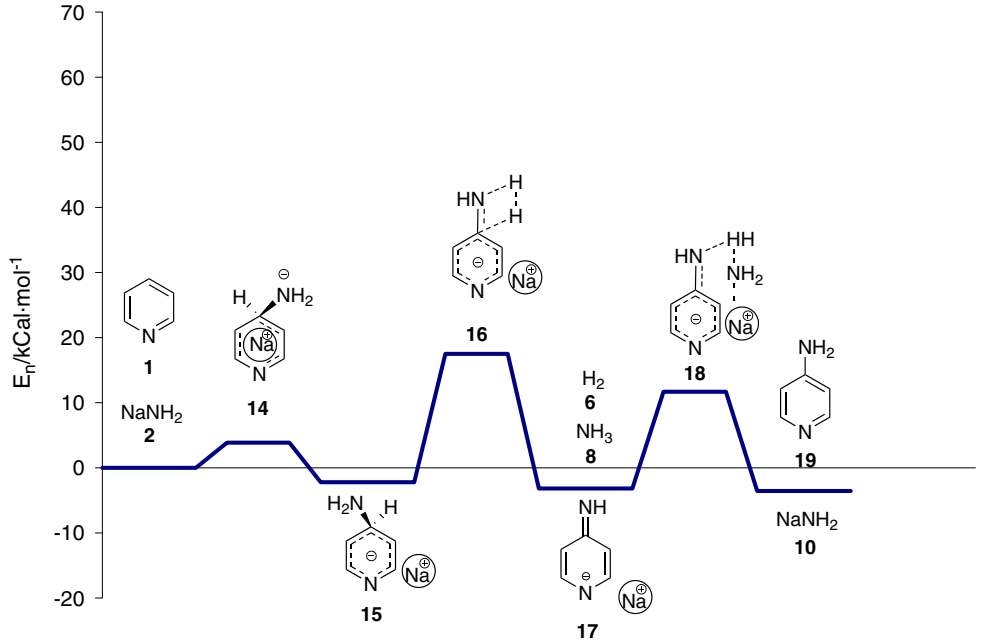

(**d**) *Mechanism 1γ trans*

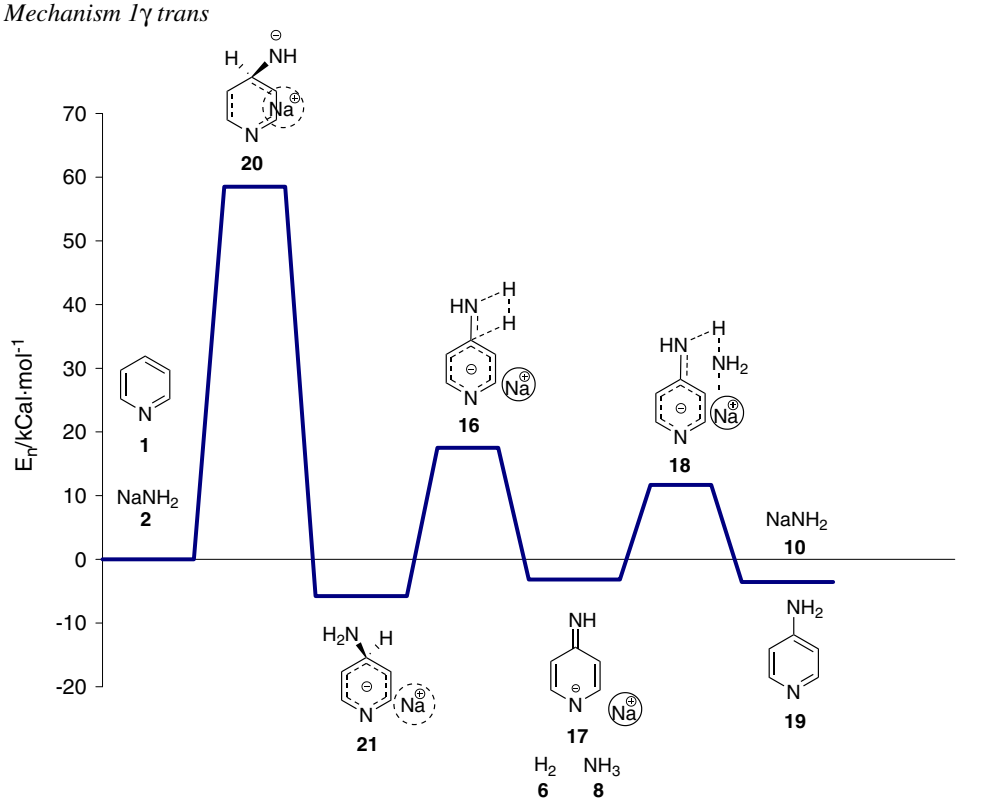

Fig. 3 (*continued*)

above and below the ring (depending on the *cis* or *trans* pathway) for these mechanistic proposals.

The first proposed mechanism occurs via an *addition and hydrogen gas elimination*. This pathway consists of three consecutive steps. When sodium amide is added to pyridine the attack is directed to either α- or γ-position. The formation of σ-complexes (**4**), (**15**), and (**21**) proceeds through transition states (TS) (**3**), (**14**), (**20**) for 1α, 1γ-*cis*, 1γ-*trans* pathways, respectively. In the elimination step, the reaction proceeds through formation of TS (**5**) and (**16**). In the case of the α-pathway, the first hydrogen atom dissociates from the carbon that is in α-position to the N, and the second one from the amide group (Scheme 1a), similarly to the γ-pathway in which the first hydrogen leaves from the carbon that is in γ-position to the N and the second one from the amide group (Scheme 1c and d). This step leads to the formation of hydrogen gas (**6**) and sodium salts (**7**) and (**17**), and is identical for the three

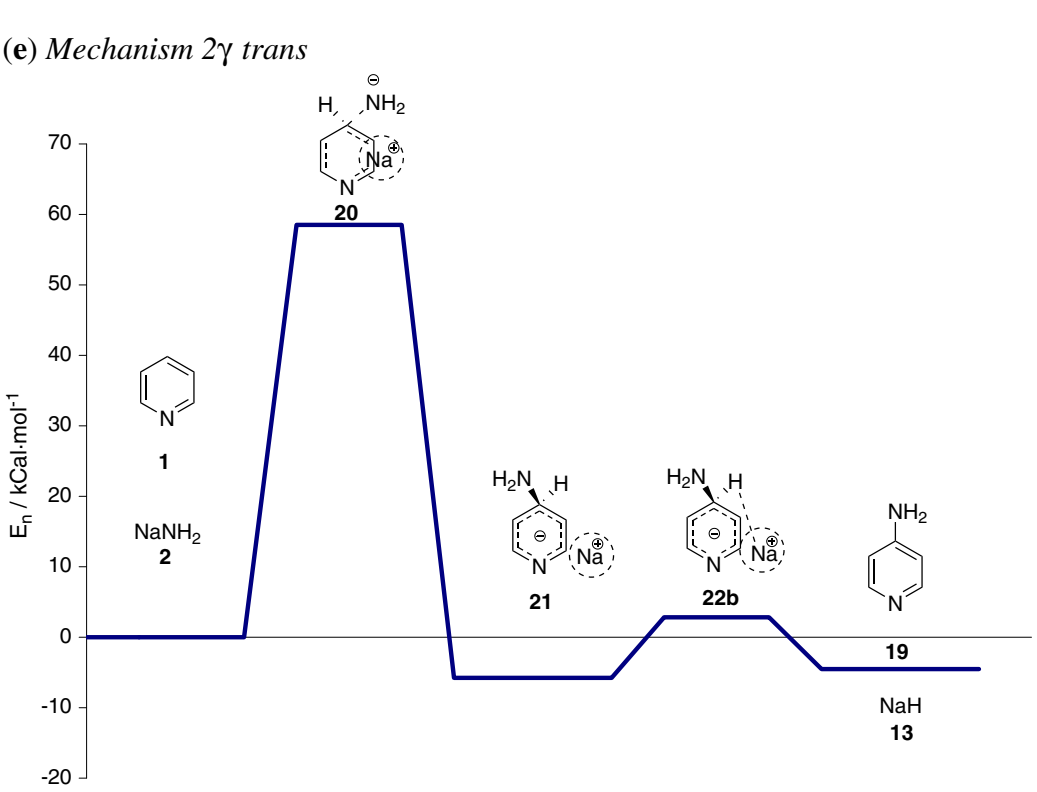

Fig. 3 (*continued*)

(Scheme 1a, c and d) pathways. Those salts later are transformed to their respective final products, α-aminopyridine (**11**) and γ-aminopyridine (**19**) and co-product sodium amide (**10**), in the concluding step.

The second proposed mechanism is *an addition and sodium hydride elimination*. While it is very similar to the first type, it is one step shorter and only contains two steps. The major difference, however, is that this pathway occurs via the elimination of NaH instead of hydrogen gas. Pathway 2γ- *cis* (Scheme 1e) was excluded from further consideration in the early stages due to the geometric arrangement of the sodium and H leaving groups. In the second (elimination) step the sodium atom and hydrogen atom that is in γ-position to the N appear on the opposite sides of the plane of the aromatic ring that makes formation of sodium hydride unfeasible.

The addition step proceeds identically to that in the first proposed mechanism. After the formation of the σ-adducts the hydrogen atom again dissociates from either alpha or gamma aromatic carbon together with sodium atom, forming TSs (**12**) and (**22b**). The pathway results in the formation of the main products α- (**11**) and γ-aminopyridine (**19**) and the co-product sodium hydride (**13**).

In order to characterize the obtained structures, we used the sum of their electronic and thermal enthalpies (SETE). We calculated activation energy barriers, E_a, as a difference between the SETE of the TS and that of the sum of the reagents, and enthalpy ΔH as a difference between the SETE of products and SETE of the reagents for each step separately. The table (Table 1) that summarizes the data contains E_a and ΔH (kCal/mol) calculated in liquid ammonia at a standard pressure of 1 atm at different temperatures.

In general, we observe a typical trend in potential energy surface diagrams that varies slightly as a function of the reaction temperature. A temperature increase of 20 K decreases the activation energy barrier by 0.01–0.60 kCal/mol and increases stability of the intermediates by 0–0.1 kCal/mol. Since the suggested experimental conditions are 1 atm and 403–423 K, we pay special attention to the reaction computed with an average experimental temperature of 413.15 K. The computed potential energy surfaces for all five pathways at 413.15 K are shown in Fig. 3.

Comparing steps 1 of all the pathways from the kinetic perspective, we observe a large activation energy barrier of 58.5 kCal/mol for the formation of the σ-complex (**20**) in both pathways progressing via *trans* γ-attack, while the E_a toward the formation of the σ-complex (**14**) resulting from the *cis* γ-attack was found to be 3.9 kCal/mol. These data unambiguously characterize the *trans* γ-addition as energetically strongly unfavorable. The activation barrier for the α-attack of pyridine is only 0.7 kCal/mol, which makes the α-attack preferable to γ-substitution, a result that is fully consistent with experimental observations [42]. However, a thermodynamic analysis gives exactly the opposite result. The most stable intermediate (**21**) is the results of the *trans* γ-addition, and is formed with −5.8 kCal/mol. The second most stable σ-complex (**15**) is produced with −2.2 kCal/mol in the *cis* γ-attack, while the least stable intermediate is (**4**) with −0.3 kCal/mol, formed as a result of the α-addition. Because the activation barrier of (**21**) is fifteen times higher that that of (**15**), pathways that start with the *trans* γ-attack (1γ- *trans* and 2γ- *trans*) are deemed as highly improbable and thus should be eliminated, regardless of thermodynamic considerations.

In the second step of the mechanism, either hydrogen gas together with intermediates (**7**) and (**17**) are formed with reaction barriers of 12.3 and 17.5 kCal/mol, respectively, or sodium hydride (**13**) and the final product α-aminopyridine (**11**) are produced with an activation energy of 24.1 kCal/mol. The overall stabilities of the intermediate products in the second step are −12.4, −0.3, and −3.7 kCal/mol for pathways 1α, 2α, and 1γ-*cis*, respectively. The analysis of this step allows us to eliminate pathway 2α, it has nearly double the activation barrier compared to the other two op-

tions and the least stability of products after the second step. While the two remaining pathways, 1α and 1γ-*cis*, are an adequate representation of the formation of both α- and γ-products, 1α mechanism is both thermodynamically and kinetically preferable because of the significantly lower activation energy barrier and more stable products formation. That conclusion is again consistent with experimental results, which report the formation ratio of the α to γ-products under the investigated conditions as 6:1.

4. Conclusions

The mechanism of the Chichibabin pyridine synthesis was investigated under homogeneous conditions using density functional theory. Earlier experimental observations were rationalized and explained. Calculations and experiments agree that the 1α pathway, being kinetically and thermodynamically most preferable among all investigated conditions, is the most reasonable mechanistic proposal to explain the formation of the dominant product, α-aminopyridine. Among the other presented pathways, 1γ-*cis* appeared the most reasonable mechanism from the energetic perspective to explain the formation of the minor product, γ-aminopyridine. While it is difficult to predict the α to γ product ratio purely based on the energetics of the reactions, both the activation energy and final product thermodynamic stability undoubtedly suggest the dominance of the α-product and thus explain the experimentally observed product ratio (6:1) in favor of this compound.

Acknowledgments

This work was supported by the University of Massachusetts Boston and in part by the National Science Foundation through TeraGrid resources at the National Center for Supercomputing Applications, TG-CHE080043N, 3/11/08–3/11/09, 30,000 SU.

Appendix A. Supplementary data

Supplementary data associated with this article can be found, in the online version, at doi:10.1016/j.comptc.2010.10.023.

References

[1] A.E. Chichibabin, O.A. Zeide, J. Russ. Phys. Chem. Soc. 46 (1914) 1216.
[2] A.E. Chichibabin, J. Russ. Phys. Chem. Soc. 37 (1906) 1229.
[3] A.N. Lomakin, Zh. Obshch. Khim. 33 (1963) 204.
[4] Y.I. Chumakov, Pyridine Bases, Kiev, Tehnika, 1965. pp. 8.
[5] T. Kametani, H. Nemoto, S. Takano, Chem. Pharm. Bull. 16 (1968) 367.
[6] R.C. Elderfield, H.E. Mertel, R.T. Mitch, I.M. Wempen, E. Werble, J. Am. Chem. Soc. 77 (1955) 4816.
[7] M.T. Leffler, Organic Reactions I, John Wiley & Sons Inc., New York, 1942. pp. 19.
[8] R.C. Elderfield, Heterocyclic Compounds I, John Wiley & Sons Inc., New York, 1950. pp. 405.
[9] C.K. Ingold, Structure and Mechanism in Organic Chemistry, Cornell University Press, Ithaca, NY, 1953. pp. 809.
[10] W. Kunz, H. Krauch, Chem. Ztg. 82 (1958) 802.
[11] L. Panzella, P. Di Donato, S. Comes, A. Napolitano, A. Palumbo, M. d'Ischia, Tetrahedron Lett. 46 (2005) 6457.
[12] B.B. Snider, B. Neubert, Org. Lett. 7 (2005) 2715.
[13] D. Xu, B. Liu, M. Zheng, J. Chem. Res. Synop. 1 (2003) 645.
[14] F. Hartner, K. Eng, Y. Hsiao, N. Rivera, M. Palucki, L. Tan, N. Yasuda, in: 35th Central Regional Meeting of the American Chemical Society, Pittsburgh, PA, United States, 19–22 October 2003 (abstracts 319).
[15] A.V. Varlamov, A.N. Levov, F. Toze, A.I. Chernyshev, V.V. Davydov, M.A. Ryabov, O.A. Egorova, Chem. Heterocycl. Comp. 38 (2002) 84 (translation of Khim. Geterotsikl. Soedin).
[16] Z. Yao, X. Gao, P. Ren, Daxue Huaxue 16 (2001) 48.
[17] M. Palucki, D.L. Hughes, N. Yasuda, C. Yang, P.J. Reider, Tetrahedron Lett. 42 (2001) 6811.
[18] E.I. Kostik, A. Abiko, A. Oku, J. Org. Chem. 66 (2001) 2618.
[19] K.G. Nazarenko, V.A. Kovtunenko, A.M. Demchenko, M. Kornilov, Yu. Ukr. Khim. Zh. (Russ. Ed.) 62 (1996) 42.
[20] R.S. Sagitullin, G.P. Shkil, I.I. Nosonova, A.A. Ferber, Khim. Geterotsikl. Soedin. 32 (1996) 147.
[21] A.S. Kiselyov, L. Strekowski, Synth. Commun. 24 (1994) 2387.
[22] A. Lichtblau, H.D. Hausen, W. Schwarz, W. Kaim, Inorg. Chem. 32 (1993) 73.
[23] T. Kawase, N. Ueno, M. Oda, Tetrahedron Lett. 33 (1992) 405.
[24] N.M. Shishlov, Sh.S. Akhmetzyanov, M.G. Zolotukhin, I.V. Novoselov, G.I. Nikiforova, A.P. Kapina, F.G. Valyamova, Dokl. Akad. Nauk SSSR 322 (1992) 304.
[25] A.V. Gulevskaya, A.F. Pozharskii, L.V. Lomachenkova, Khim. Geterotsikl. Soedin. 11 (1990) 1575.
[26] I. Liepina, M. Sile, R.A. Karakhanov, A. Avots, Latv. PSR Zinat. Akad. Vestis Kim. Ser. 4 (1989) 433.
[27] I. Liepina, V. Slavinska, M. Sile, A. Avots, R.A. Karakhanov, Latv. PSR Zinat. Akad. Vestis Kim. Ser. 3 (1989) 339.
[28] C.K. McGill, A. Rappa, Adv. Heterocycl. Chem. 44 (1988) 1.
[29] I. Liepina, M. Sile, V.A. Slavinskaya, A. Avots, Latv. PSR Zinat. Akad. Vestis Kim. Ser. 3 (1988) 327.
[30] I. Liepina, M. Sile, V.A. Slavinskaya, A. Avots, Latv. PSR Zinat. Akad. Vestis Kim. Ser. 2 (1988) 149.
[31] D.J. Buurman, H.C. Van der Plas, J. Heterocycl. Chem. 24 (1987) 1377.
[32] H.C. Van der Plas, Khim. Geterotsikl. Soedin. 8 (1987) 1011.
[33] K. Breuker, H.C. Van der Plas, A. Van Veldhuizen, Isr. J. Chem. 27 (1986) 67.
[34] H.C. Van der Plas, M. Wozniak, Croat. Chem. Acta 59 (1986) 33.
[35] A. Rykowski, H.C. Van der Plas, Synthesis 9 (1985) 884.
[36] Y. Ma, S. Breslin, I. Keresztes, E. Lobkovsky, D.B. Collum, J. Org. Chem. 73 (2008) 9610.
[37] N.N. Polygalova, A.G. Mikhailovskii, E.V. Vikhareva, M.I. Vakhrin, Chem. Heterocycl. Compd. 43 (2007) 900.
[38] S.R. Breslin, D.B. Collum, in: 35th Northeast Regional Meeting of the American Chemical Society, Binghamton, NY, United States, 5–7 October 2006.
[39] L.K. Montgomery, J.C. Huffman, E.A. Jurczak, M.P. Grendze, J. Am. Chem. Soc. 108 (1986) 6004.
[40] H. Tondys, H.C. Van der Plas, M. Wozniak, J. Heterocycl. Chem. 22 (1985) 353.
[41] K.-L. Wang, W.-T. Liou, D.-J. Liaw, W.-T. Chen, Dyes Pigments 78 (2008) 93.
[42] J. Breuker, H.C. Van der Plas, Recl. J. R. Neth. Chem. Soc. 102 (1983) 367.
[43] V.N. Novikov, A.F. Pozharskii, V.N. Doronkin, Chem. Heterocycl. Compd. 12 (1976) 210.
[44] R.A. Abramovitch, F. Helmer, J.G. Saha, Can. J. Chem. 43 (1965) 725.
[45] V.N. Novikov, A.F. Pozharskii, V.N. Doronkin, Khim. Geterotsickl. Soedin. 2 (1976) 244.
[46] M.J. Frisch et al., Gaussian03, Revision E.01, Gaussian Inc., Wallingford, CT, 2004.
[47] C. Catlett, W.E. Allcock, P. Andrews, R. Aydt, R. Bair, N. Balac, B. Banister, in: L. Grandinetti (Ed.), HPC and Grids in Action, Advances in Parallel Computing, IOS Press, Amsterdam, 2007.
[48] K.K. Irikura, R.D. Johnson III, R.N. Kacker, J. Phys. Chem. A. 109 (2005) 8430.
[49] R.N. Akhvlediani, V.P. Shabunova, I.A. Morozova, T.A. Volodina, N.N. Suvorov, Zh. Org. Khim. 17 (1981) 1542.